PROTEINS: Structure, Function, and Genetics 29:15–31 (1997)

Structure of Soybean Lipoxygenase L3 and a Comparison With Its L1 Isoenzyme

Ewa Skrzypczak-Jankun,[1]* L. Mario Amzel,[2] Beth A. Kroa,[1] and M.O. Funk, Jr.[1]
[1]*Department of Chemistry, The University of Toledo, Toledo, Ohio*
[2]*Department of Biophysics and Biophysical Chemistry, Johns Hopkins University School of Medicine, Baltimore, Maryland*

ABSTRACT **Soybean lipoxygenase isoenzyme L3 represents a second example (after L1) of the X-ray structure (R = 17% at 2.6 Å resolution) for a member of the large family of lipoxygenases. L1 and L3 have different characteristics in catalysis, although they share 72% sequence identity (the changes impact 255 amino acids) and similar folding (average Cα rms deviation of 1 Å). The critical nonheme iron site has the same features as for L1: 3O and 3N in pseudo C_{3v} orientation, with two oxygen atoms (from Asn713 and water) at a nonbinding distance. Asn713 and His518 are strategically located at the junction of three cavities connecting the iron site with the molecule surface. The most visible differences between L1 and L3 isoenzymes occur in and near these cavities, affecting their accessibility and volume. Among the L1/L3 substitutions Glu256/Thr274, Tyr409/His429, and Ser747/Asp766 affect the salt bridges (L1: Glu256...His248 and Asp490...Arg707) that in L1 restrict the access to the iron site from two opposite directions. The L3 molecule has a passage going through the whole length of the helical domain, starting at the interface with the N_t-domain (near 25–27 and 254–278) and going to the opposite end of the C_t-domain (near 367, 749). The substrate binding and the role of His513, His266, His776 (and other residues nearby) are illustrated and discussed by using models of linoleic acid binding. These hypotheses provide a possible explanation for a stringent stereospecificity of catalytic products in L1 (that produces predominantly 13-hydroperoxide) versus the lack of such specificity in L3 (that turns out a mixture of 9- and 13-hydroperoxides and their diastereoisomers). Proteins 29: 15–31, 1997.**

Key words: metalloprotein; lipoxygenase; X-ray structure; fatty acid; electron transfer

INTRODUCTION

Lipoxygenase catalysis is a central element in polyunsaturated fatty acid metabolism in both plants and animals.[1] Plant lipoxygenases are all large (M_r approximately 95 kDa) monomeric polypeptides with closely related primary structures. Mammalian lipoxygenases are typically smaller than their plant counterparts with M_r approximately 75 kDa. Maximum sequence overlap* is obtained between the mammalian enzymes and the C-terminal portion of the plant enzymes. All lipoxygenases have a common cofactor, which is a single nonheme iron atom. Spectroscopic studies (EPR, Mossbauer, MCD and EXAFS), principally conducted on soybean lipoxygenase-1, have provided evidence for a redox role for the iron in the catalytic mechanism,[2] pointing toward a six-coordinate, essentially octahedral environment for the iron atom.[3] Furthermore, there is experimental evidence that water is one ligand to the iron in the ferric, iron(III) form of the enzyme.[4,5] The only known and fully described three-dimensional (3D) structure of lipoxygenase comes from soybean. In the X-ray analyses performed for the ferrous, Fe(II) form of soybean lipoxygenase-1,[6,7] the iron cofactor was found to be buried and surrounded by three histidines, C-terminal isoleucine, asparagine, and water. Two of its potential ligands (asparagine and solvent molecule) were located at a nonbinding distance.

*The sequences of 20 plant and 13 mammalian lipoxygenases listed in GenBank (January 1997) were aligned and taken into consideration. The authors thank Jeffrey A. Kramer from Wayne State University for his valuable assistance in searching the database and doing the sequence alignments of these enzymes. The abbreviations refer to the source and are as follows: (a) plant enzymes: *arabido1*, *arabido2*, *barley1*, *cuke1*, *kbean*, *lentil*, *pea1*, *peacyto*, *peaseed*, *potatA*, *potatB*, *rice2*, soybean *Hawkeye cv.*: *soyL1*, *soyL2*, *soyL3*, soybean *Provar cv.-soyP4* (=L3 except for 5 residues, all these soybean enzymes were called L1, L2, and L3 through the text), *soywil*, *tobac1*, *tomat1*, and *tomat2*, (b) mammalian enzymes: *human5*, *mouse5*, *rat5*, *syrham5*, *bovine12*, *human12*, *mouse12*, *musplat12*, *porcine12*, *rat12*, *musepi*, *human15*, *rabbit15* (list of aligned sequences and full references may be obtained from E.S.J.) The other abbreviations used in the text: RT, room temperature; LT, low temperature; FA, fatty acid; Wat, water.

Contract grant sponsor: NIH; Contract grant numbers: GM-46522 and GM-44692.
Present address: Beth A. Kroa, Chemistry Department, Kutztown State University, Kutztown, PA 19530.
*Correspondence to: Ewa Skrzypczak-Jankun, Department of Chemistry, The University of Toledo, Toledo, OH 43606.
E-mail: ejankun@uoft02.utoledo.edu
Received 1 November 1996; Accepted 10 April 1997

The catalyzed reaction involves the regioselective and stereoselective oxygenation of polyunsaturated fatty acids. In animals, the action of lipoxygenase on arachidonic acid initiates the biosynthesis of several families of metabolites with important physiological activities. Because certain end products of this metabolism have proinflammatory effects (e.g., leukotriene B4), the lipoxygenase pathway has become an important therapeutic target in diseases with an inflammatory component.[8] In plants, lipoxygenase acts on arachidonic, linoleic, and linolenic acids, and the result is the formation of a variety of compounds, some of which have growth regulatory or pest resistance properties.[9] Although the catalytic mechanism of all lipoxygenases may be the same,[3] there are significant differences in the properties of the plant and animal enzymes. For example, the soybean enzyme is a soluble, cytosolic protein, whereas the 5-lipoxygenase from rat and human leukocytes is activated by binding to a specific membrane associated activating protein.[10] Therefore, although it is highly likely that the lipoxygenases all employ the same catalytic mechanism, there is significant variation among them in the regulation of the activity of the enzyme from different organisms. The most widely studied plant lipoxygenase from soybean exists in the form of several isozymes sharing approximately 70% of sequence homology. Soybean lipoxygenase isozymes L1, L2, and L3 have significantly different properties.[11] For example, L1 has a broad pH optimum extending to pH $>$ 9 that is not shared by the other soybean isoenzymes. L1 also shows a much higher degree of regioselectivity and stereoselectivity in comparison with L3. The studies of stereochemistry of the fatty acid hydroperoxide products of soybean lipoxygenase catalysis[12,13] provide the evidence that the soybean isoenzymes differ in this aspect of catalysis. L1 acting on linoleic or arachidonic acid produces predominantly 13-hydroperoxy-9-*cis*,11-*trans* products, with 13R:13S approximately 10:90. L3 delivers a mixture (50:50) of 9- and 13-hydroperoxides showing a preference for *cis-trans* vs. *trans-trans* dienoic system (approximately 60:40) and with higher turn out of R stereoisomers over S (approximately 60:40).

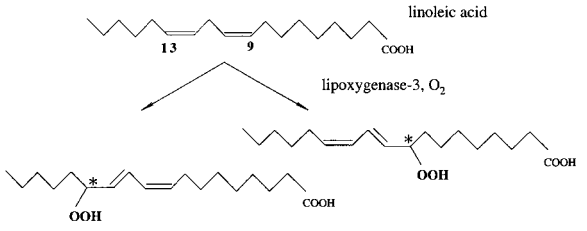

mixture of: 13- or 9-hydroperoxides, *cis-trans* or *trans-trans* dienoic system, * R or S

Comparison of the 3D structures of the two proteins will presumably make it possible to account for these differences in the biological properties.

The X-ray studies of lipoxygenase-1 were conducted exclusively on enzyme from soybeans, *cv. Hawkeye*. This work concerns lipoxygenase-3 or L3 from soybeans, *cv. Provar*. We previously reported a preliminary characterization of L3 crystals[14,15] and a preliminary structure.[16] This report contains a description of the 3D structure of L3 isoenzyme, a comparison with the structure of L1, and a new hypothesis of substrate binding illustrated by modeling linoleic acid into the L3 structure and based on an assumption of a long-range electron transfer.

MATERIALS AND METHODS

Isolation, Purification, and Crystallization

Soybean seeds, *cv. Provar*, were ground and defatted by using hexane. The dried meal was stored in a freezer. The lipoxygenase isoenzymes were extracted and purified by using chromatofocusing.[17] The purified protein was dialyzed against Tris HCl buffer (0.1 M, pH 7.0) and concentrated (Minicon 30, Amicon). The protein concentration was determined by using a molar absorption value of 118,000 L $mol^{-1}cm^{-1}$ for 280 nm.[11] Only freshly isolated protein was used for crystallization. The crystals used for data collection grew from a mixture of the following: L3 (10 mg/mL in 0.1 M Tris HCl, pH 7.0), 20% PEG 8000 (w/v, in 0.05 M sodium citrate-phosphate buffer, pH 4.6, 0.2% NaN_3, w/v), 0.1 M sodium phosphate buffer, pH 7.0, and water, in a 3:6:1:2 ratio, seeded and equilibrated against 20% PEG 8000. The pH of the crystallization mixture was 5.3 throughout the experiments. Seeds were prepared from the previous crystallization by crushing several of the best available crystals in approximately 50 µL of 10% PEG 8000 (w/v) by using a Pellet Pestle Mixer. The crushed particles were diluted 1:10,000 and added to the crystallization mixture in a 1:200 ratio. The crystals were grown in batch mode combined with slow evaporation, where the "sitting drop" was from 600 to 1200 µL and the reservoir of PEG solution was 3–5 mL. This was done in small, concentric beakers cut to 10 and 15 mm in height. The larger beaker was covered with a glass plate and sealed with silicone grease. The crystallizations were conducted at 23°C in an incubator. The crystals appeared within 2 days and stopped growing after several days. The typical crystals of soybean lipoxygenase L3 were 0.5–0.7 mm long and 0.05–0.3 mm in the cross-sectional dimensions.

Soybean seeds were provided by Dr. John Thompson, USDA Plant and Soil Nutrition Laboratory, Ithaca, New York. Histidine, sodium phosphates, Tris base, Tris HCl, sodium citrate, and Pellet Pestle Mixer were purchased from Fisher Scientific, PEG 8000 from Fluka or Sigma, sodium azide from Al-

drich, and Polybuffer 74 from Pharmacia. All solutions were filtered prior to crystallization through Nalgene 0.22 μm acrylic syringe filters.

Data Collection

Crystals approximately 0.5 × 0.2 × 0.1 mm were mounted in Φ1.0-mm glass capillaries and screened on an area detector for intensity, resolution, and mosaicity. All examined crystals showed excellent agreement in unit cell dimensions (within 1 σ). The crystals diffracted to 2.1 Å but decayed rapidly and showed very little data beyond 2.5 Å resolution. To reduce decay and achieve the best possible completeness, the data were collected on two crystals and trimmed to 2.6 Å resolution only. All intensity measurements were done at room temperature[16] on an R-AXIS II imaging plate detector, using graphite monochromatized CuKα radiation from the 0.3 × 0.3-mm source of a Rigaku RU200 rotating anode generator operating at 50 kV and 100 mA. Crystal data: monoclinic, C2, a = 112.8(1) Å, b = 137.4(1) Å, c = 61.85(3) Å, β = 95.50(5)°, one molecule of L3:Fe(II) per asymmetric unit that corresponds to 50% protein and 2.46 kDa/Å^3 in the crystal. The data (74,331 reflections measured) from two crystals were combined, reduced, and scaled together by using the R-AXIS II processing software, providing 23,403 independent reflections with $I > 2\sigma(I)$, R_{merge} = 6.2% (on I), and 80.1% completeness of the data (48% in the last shell from 2.75 to 2.6 Å).

Structure Solution and Refinement

The structure was solved by molecular replacement using the program A.Mo.Re,[18] 10,799 reflections from 10 to 3.5 Å resolution and 5462 atoms from soybean lipoxygenase L1 as a model. Because the domains of the enzyme might have been in a different relative orientation in L3 than in L1, the N_t-domain was excluded from the starting model to avoid possible bias. The L1 atomic coordinate file (entry 1SBL in the Brookhaven Protein Data Bank) was truncated to include residues Asn146 to Ile839 and Fe. These coordinates were then further edited (deletions and mutations) to include only the atoms that were common to both L1 and L3 molecules. The rotation search brought a single solution with a peak height of 22σ (where σ = rms deviation) above the average (next highest peak 5σ). The translation search gave very clear solution as well, with a peak height 10σ above the mean (next peak, 3σ). The rotation search with the N_t-domain only did not give a clear answer, but the solution for both domains combined was similar to the one that was obtained for the C_t-domain alone. This observation indicated that the general topology of the L3 molecule might be very close to L1. Refinement of the orientation and position of the molecule using A.Mo.Re increased the correlation coefficient from 0.37 to 0.52 and reduced the discrepancy factor to 0.41. This solution was used to transform the coordinates of the model into the unit cell of the L3 molecule, and the calculations were continued by using X-PLOR.[19] The rigid body refinement was performed without the N_t-domain, and the $2F_o$-F_c map was examined to see if the missing domain could be located. The answer was positive so the rigid body refinement was repeated, and the map was recalculated by using 784 residues from both domains and reflections from 8 to 2.8 Å resolution (19,239 reflections, $F > 3\sigma(F)$). At this stage (73 residues and 566 nonhydrogen atoms from mutated side chains still missing) a $2F_o$-F_c map (R = 0.40) was used to manually refit the entire model. The sites of deletions, insertions, and mutations with drastic changes in the size of the side chain (Lys to Val, Ser or Gly to Lys, Gln to Pro, Pro to Trp, Thr to Arg, etc.) were examined first to evaluate the quality of the map, which was found to be exceptionally good. Missing residues and side chains were built in whenever possible, and this new, expanded (805 residues) model ($B_{overall}$ = 25.0, R = 0.39) served as a starting point for refinement. All model building and iterative refitting to the maps in the course of refinement were conducted by using the program CHAIN.[20] Fragments at the N_t-end with broken connectivity (first β-strand) and residues without definite electron density for the side chains were kept as Gly or Ala during refinement until the electron density map indicated clearly the shape and connectivity direction of the missing atoms. That was especially important in the case of the N_t residues, because it was not clear which of the first 50 amino acids belonged to the first strand in the β-barrel. Simulated annealing, omit maps, and R-free (10% of the data) were used as a cross-validation of the model. The structure was refined to R = 18% with data extending to 2.6 Å resolution. At this stage the maps were examined for the existence of possible water molecules in the internal cavities and surface crevices. Water molecules (170) were included in the refinement with the starting B of 35 Å^2. Their occupancies were not refined.

The distances and angles involving iron were defined in a topology file and included in the refinement, except for the angles between the ligands opposite to one another. All force constants were assigned 0 and kept this way for the first two rounds of model building, so as not to impose any geometrical constraints on the possible ligands of iron. The force constants were gradually increased to bring the model closer to the bond distances expected on the basis of the literature data.[21] The target parameters for distances and angles involving iron were as follows: Fe-O 2.1 Å, Fe-N 2.2 Å, O(N)-Fe-N(O) 90° for

the neighboring ligands, with force constants of 270 kcal/mol-Å^2 for distances and 50 kcal/mol-rad^2 for angles. The following residues in the vicinity of iron were tested as possible ligands: His518, His523, His709, Asn713, terminal carboxyl from Ile857, and a solvent molecule, tentatively assigned as water Wat901. Although all of them could be positioned at the binding distance to iron, the shape of the electron density omit maps clearly indicated that the side chain of Asn713 should be turned further away from iron, and the peak for the solvent molecule stayed beyond 3 Å from iron even when this molecule was defined as ligand. Consequently to these observations, the definitions for bonds and angles involving Asn713, Wat901, and iron were excluded from the topology file and these two residues were refined as having only nonbonded interactions with iron cofactor.

The final results correspond to R = 17% (R-free(10% reflections) = 26%) for 22,440 reflections ($F_o > 2\sigma(F)$, 8–2.6 Å resolution) and 6867 nonhydrogen atoms that comprise 836 amino acids (of 857), the iron cofactor, and 170 water molecules. The 21 missing residues are: the first eight residues from the N-terminus and 13 residues (from residue 33–45) comprising a loop located after the first β-strand and referred to hereafter as an insertion loop. The insertion loop has been represented in some of the diagrams (see Figs. 2, 3) in an arbitrary conformation to show its location within the molecule and to give an indication of its size. The rms deviations from ideality of the model are 0.015 Å for bond distances and 3.6° for bond angles. The average temperature factor for all atoms of 31 Å^2 reflects the high temperature factors of the external loops that show much higher values than the bulk of the molecule.

RESULTS AND DISCUSSION

Quality of the Model and General Structural Features

Crystals of soybean lipoxygenase have a short shelf life and were reported to show inconsistent results in X-ray diffraction experiments, suggesting some kind of heterogeneity.[22,23] The L3 form of lipoxygenase in the native or iron(II) state was purified by a chromatofocusing procedure that cleanly resolved all lipoxygenase isoenzymes, eliminating any *biological* microheterogeneity of the protein. Freshly purified samples of L3 were found to provide better crystals with good diffraction characteristics compared with solutions stored at 4°C for even a few days. It was also found to be necessary to collect X-ray diffraction data promptly on the crystals once they stopped growing (not more than 2 weeks from the crystallization setup) and to keep them covered with solvent during data collection. The diminished quality of the diffraction from older or drier crystals caused not only a reduction in intensity and resolution but also difficulties in data indexing. Similar observations have been noted in a preliminary characterization of L3 crystals with the same unit cell and space group, but obtained under different crystallization conditions (sodium acetate, PEG3400, pH 5.7). The diffraction data were collected by using synchrotron radiation to 3 Å resolution and 61% completeness.[24] This independent study confirms our earlier observations and indicates that the difficulties might be associated with the nature of this molecule and the way it packs into a crystal lattice. The problems are related to the presence of very large channels in the crystal lattice that might be a source of fluctuation in solvent distribution and/or *structural* heterogeneity of the molecules. This view was supported by observations at low temperatures, where the crystals were found to go through a transition that produced a new space group, a 10% reduction in the volume of the unit cell, and a superlattice reflecting the periodic arrangement of the molecules and solvent channels.[23] Figures 1[†] and 2 show the folding, different domains, and a secondary structure notation[‡] for the L3 molecule. To better visualize the different segments, the molecule can be divided into five regions (roughly: green = 1:9–190, yellow = 2:191–254, red = 3:255–345, blue = 4:346–488, gray = 5:489–857) and three cavities connecting the iron site with the protein surface. The electron density map for the L3 model, very clear and well defined for the majority of residues, shows a few gaps and indicates possible multiple conformations not only for the side chains but also for the main chain of a few peripheral loops (Pro169-Pro173 in E8→H1, cisPro384-Gln400 in E12→H7, Pro472-Asp477 in E15→E16, and Glu625-Tyr627 preceding H15). Similar observations were made for the L1 structure studied at room temperature,[6] and the effect did not subside even at 100 K,[7] suggesting that *dynamic* disorder may lead to *statistical* disorder in frozen crystals. Therefore, limited *structural heterogeneity*

[†]The illustrations have been made by using programs MOLSCRIPT (Kraulis, P.J. J. Appl. Crystrallogr. 24:946–950, 1991), CHAIN,[20] and InsightII (User Guide, Release 95.0, Biosym/MSI, San Diego, CA).

[‡]L3 secondary structure assignments (Fig. 2,[25]) follow the ordering introduced for L1[6]: α-helices = H, β-strands = E, an arrow "→" is used in the text to denote a loop of the polypeptide chain between two secondary structure elements (i.e., E8→H1, etc.) or a fragment between two given residues (189→201, etc.), numbering of the secondary structure elements after L1: 11–20(E1), 21–24(H), 58–64(E2), 76–81(E3), 96–104(E4), 112–119(E5), 125–133(E6), 141–149(E7), 159–162(E8), 174–178(H1), 204–205(E), 273–293(H2), 235–236(E), 304–308(H3), 319–322(H4), 336–337(E10), 343–344(E11), 361–370(H6), 378–379(E12), 415–420(H7), 424–428(E13), 434–440(H8), 450–456(E14), 462–472(E15), 481–486(E16), 492–536(H9, internal π–helix 516–520), 542–547(H10), 554–564(H11), 571–575(H12), 582–590(H13), 600–606(H14), 610–612(E), 620–622(E), 628–649(H15), 655–659(H16), 662–673(H17), 693–720(H18), 740–747(H19), 749–756(H20), 760–773(H21), 795–820(H22).

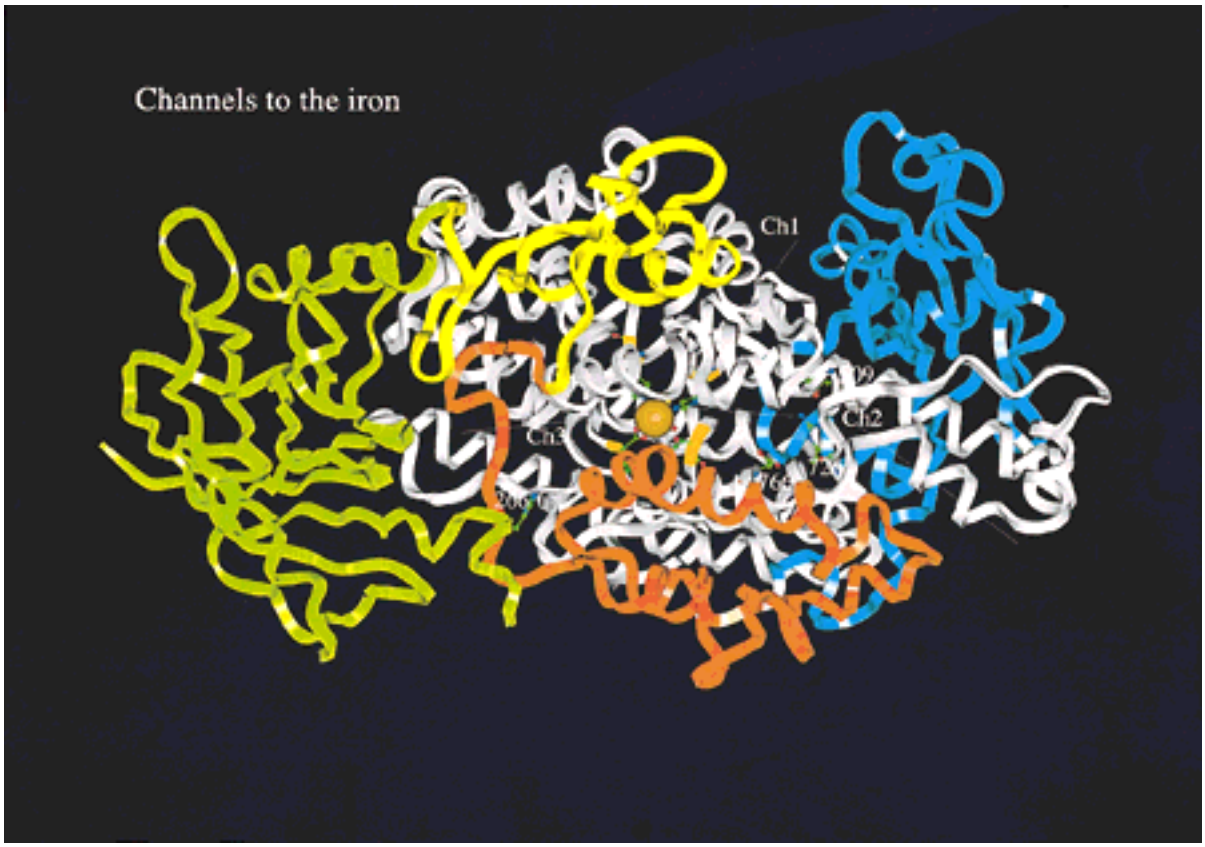

Fig. 1. Ribbon drawing of L3 colored to show different regions: green = 1:9–190, yellow = 2:191–254, red = 3:255–345, white = proline triad 346–348, blue = 4:349–488, gray = 5:489–857. Ch1, Ch2, Ch3 mark the directions of the three passages to Fe atom represented by a ball of 2 Å radius.

might be a common feature in lipoxygenase structural X-ray analysis.

Sequences published for L3[26,27] correspond to two soybean cultivars that show differences at five positions (*cv. Provar* followed by *cv. Hawkeye*): Ser57Pro, Pro112Leu, Ile201Val, Asp382Glu, and Asp428Gly.[26] All of the assignments deduced from the cDNA sequence for the L3 from *cv. Provar*[26] were confirmed by the X-ray structure. Relative to the L1 sequence (839 residues), L3 (857 residues) has amino acid deletions at 7 positions, insertions at 25 positions, and different amino acids at 223 positions. Some deletions (3) and most of the insertions (21) were found in the N-terminal region and in the insertion loop between β-strands 1 and 2. The other 4 deletions and 4 insertions were located in the loops: coils between H1 and H2, before H7, after H8, in H13, and after H22 (the position of H23 in L1). Therefore, the deletions (3) and insertions (21) were all located on the surface of the molecule or in the parts of the enzyme of no definite secondary structure. Other differences, however, are spread throughout the molecule and affect both well structured β-sheets and helices, as well as random coil fragments. Of 37 secondary structure elements, common for L1 and L3, only 6 β-strands (E1, 2, 5, 8, 9, and 14) and 2 helices (H10 and H14) are not affected by mutations. E9, H5, and H23, defined in L1, are not observed in L3. In general, for approximately 70% identity, one might expect approximately 90% conservation of the secondary structure and a 1 Å rms deviation between Cα atoms of the superimposed molecules.[28] L1 and L3 soybean lipoxygenases comply to that showing a close agreement of Cα backbones with an average shift between Cα's of 1 Å. The greatest differences are observed in the flexible loops regions and near the cavities leading to the iron site. There are two pairs of short antiparallel β-strands in L3 that were not defined in L1—one next to H11 (204–205 and 235–236) and another between H14 and H15. Also, both ends of the disordered insertion loop show some helical features, indicating a possible, additional helix in the N-terminal domain of the L3 structure.

It is worth noticing that four β-strands, E13 through E16, together with the long, pin-like loop

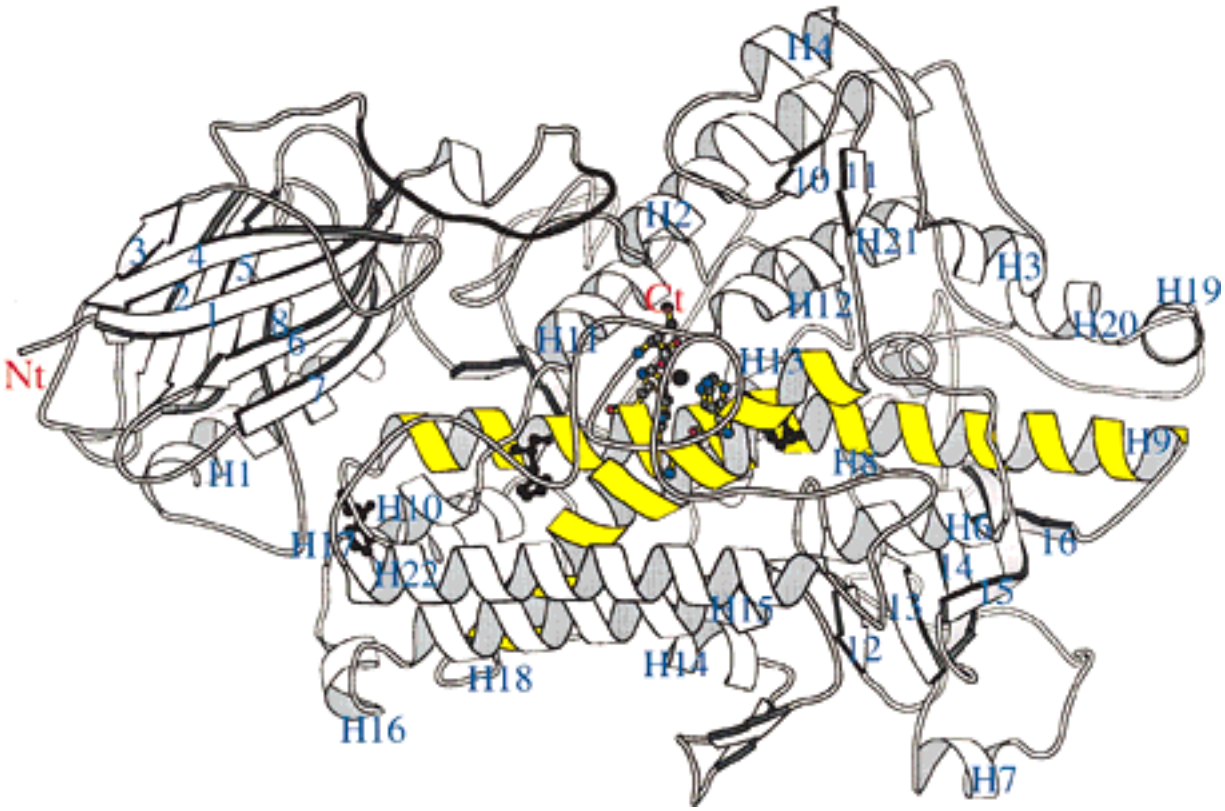

Fig. 2. Ribbon drawing of lipoxygenase L3 showing the numbering of the secondary structure elements, notation as for L1 after Boyington et al., 1993. The β-strands are marked with Arabic numbers, the helices (H) are marked at their N-terminal ends. Fe, H518, H523, H709, N713, I857, Wat901, and three other conserved histidines H513, H541, H550 are marked in black as ball-and-stick models (missing residues marked in arbitrary positions as a black coil between the first two β-strands).

(residues cisPro384 to Thr402) between E12 and H7, form a six stranded, barrel-like feature, similar to the eight stranded barrel of the N_t-domain at the opposite end of the molecule (Fig. 3a). The H7 helice and the immediately preceding coil (residues approximately 405–414) are topologically similar to the insertion loop and the helical fragment located after E1, at the end of the N_t domain (next to cavity III). Also, in proximity to this six-stranded, barrel-like feature there is a flap formed by H14 and the two following β-strands, that resembles the H4-E10-E11 fragment located near the E1-E8 barrel, at the opposite side of the molecule. It has been noticed that β-barrels are essential in lipid binding proteins.[7,29] There is an indication that the N-terminal barrel is indispensable for catalysis in soybean lipoxygenase.[30] The two topological motifs highlighted in Figure 3a might be, therefore, relevant to molecular recognition in catalysis and/or proteolysis of these enzymes.

The 3D structure provides additional insights into previously reported observations on lipoxygenase in limited proteolysis experiments.[31,32] Trypsin cleaved L3 into a large C-terminal fragment (M_r = 60 kDa) and a small N-terminal fragment (M_r = 37 kDa). Separation of the fragments required partially denaturing conditions. Furthermore, neither of the isolated fragments ever displayed catalytic activity, and reconstitution of active enzyme from the resolved fragments was never achieved. The protein is cleaved after Arg336 (beginning of E10, Fig. 3b), located on the surface in an exposed hair pin, and the N-terminal fragment, therefore, ends after H4. Although the iron site is buried deeply inside the molecule, when the N-terminal fragment is removed, one side of the coordination sphere becomes exposed to the solvent. Trypsin cleavage alone would not be expected to result in a significant change in the conformation because the secondary structural elements, including H2 through H4, are connected to the others by a tightly woven network of hydrogen bonds. Denaturation to the extent that the two fragments could be separated from each other would also be expected to expose the iron-binding site and lead to conformational changes through loss of the hydrogen-bonding

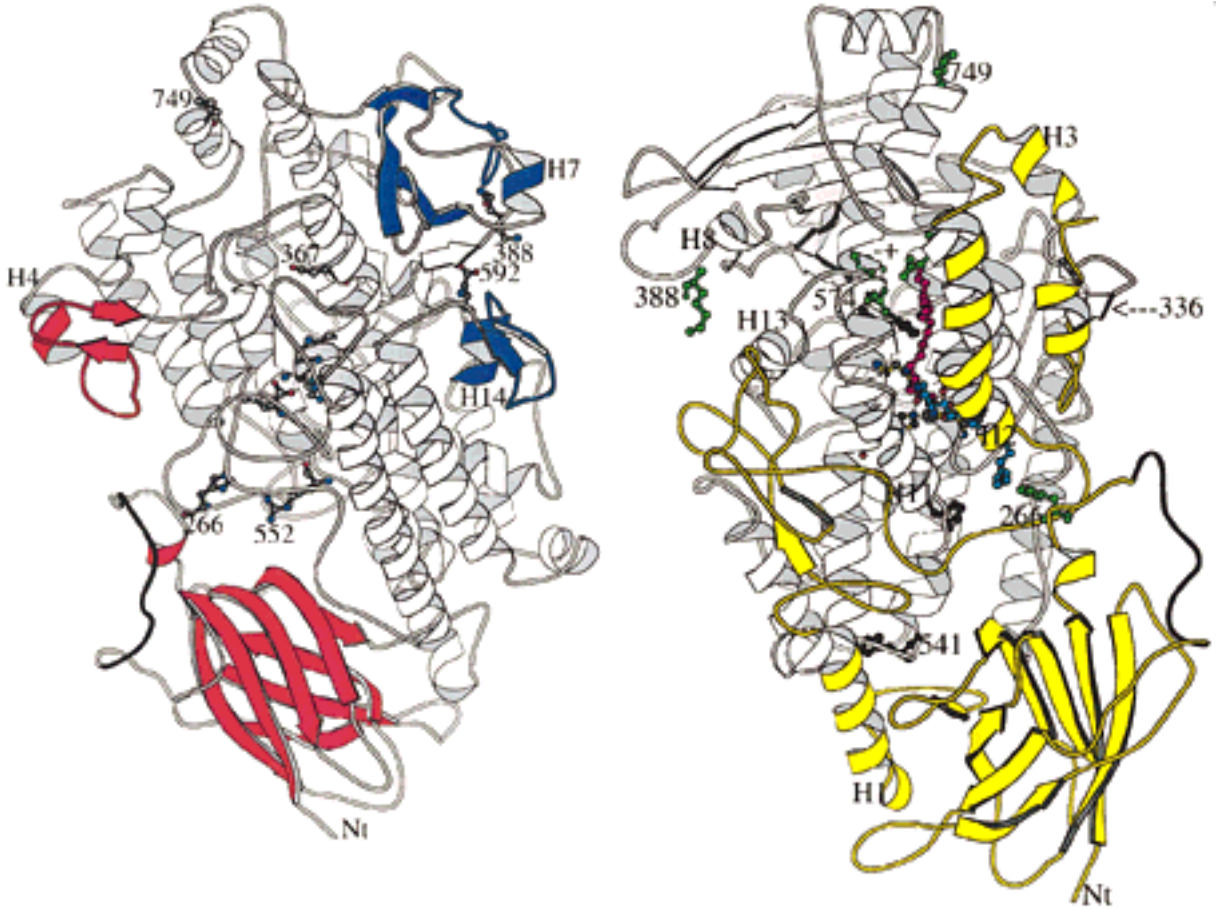

Fig. 3. Ribbon drawings of L3: **a** (left): Chosen topological features, colors red and blue correspond to the ''oxygen'' and ''nitrogen'' sides of the iron coordination sphere. Residues His266, Arg552, Lys388, Asp592 and Pro749 and Glu367 marked the cavities I, II, and III. The β-strands E13, 14, 15, and 16 and the long pin-like coil between E12 and H7, form a β-barrel like feature, viewed here down its vertical axis. **b** (right): ''Top view,'' marked in yellow is N_t to Arg336 fragment, 336–337 is a scissile bond for trypsin-like proteases. Chosen residues to mark the channels—green, purple, and light blue models— correspond to the modeling of linoleic acid binding at two different orientations.

network. This would account for the loss of catalytic activity upon fragment separation and the lack of success of reconstitution experiments.

Iron-Binding Site

The iron-binding site of the L3 molecule consists of iron(II), its four ligands, and two potential ligands (Fig. 4), providing 3O and 3N atoms. The nitrogens are NE2 atoms from three histidines, two provided by H9 (518 and 523) and one from H18 (709). The liganded oxygen comes from the C-terminal carboxyl of Ile857 (OT2), and two additional oxygens are provided by Asn713 (OD1) and a water molecule (O901). The geometric distribution of these atoms indicates an octahedral coordination of iron with a distorted C_{3v} symmetry, where oxygens and nitrogens are grouped at the opposite ends of a pseudo threefold axis. The average distances and angles are: Fe-N 2.2, Fe-O 2.1 Å (only OT2 Ile857), N-Fe-N 87°, N-Fe-O 84°, and O-Fe-O 105°. The distortion results from the fact that two oxygens are further away from iron (3.0 Å) than the other ligands (Fig. 4a). Asp713 and the water molecule are not covalently bound to iron, yet they can be brought to a bonding distance without any disturbance to their environment. The side chain of Asn713 participates in an extensive hydrogen-bonding network (Table I), whereas water 901 is sitting in a large, hydrophobic cavity (Fig. 5) and, in this model, is not involved in any other than van der Waals interactions. The nitrogen side of the iron coordination sphere is buried in the groove between H9 and H18 and isolated from the surface by the H13→H15 fragment of the molecule (Fig. 3a). The oxygen side is flanked by H11 and H21 and separated from the solvent region by H2 (Fig. 3b). The iron atom and the residues surrounding it in the L3 structure are shifted by 0.3–0.9 Å, in comparison with L1, toward the cleft between helices H11 and

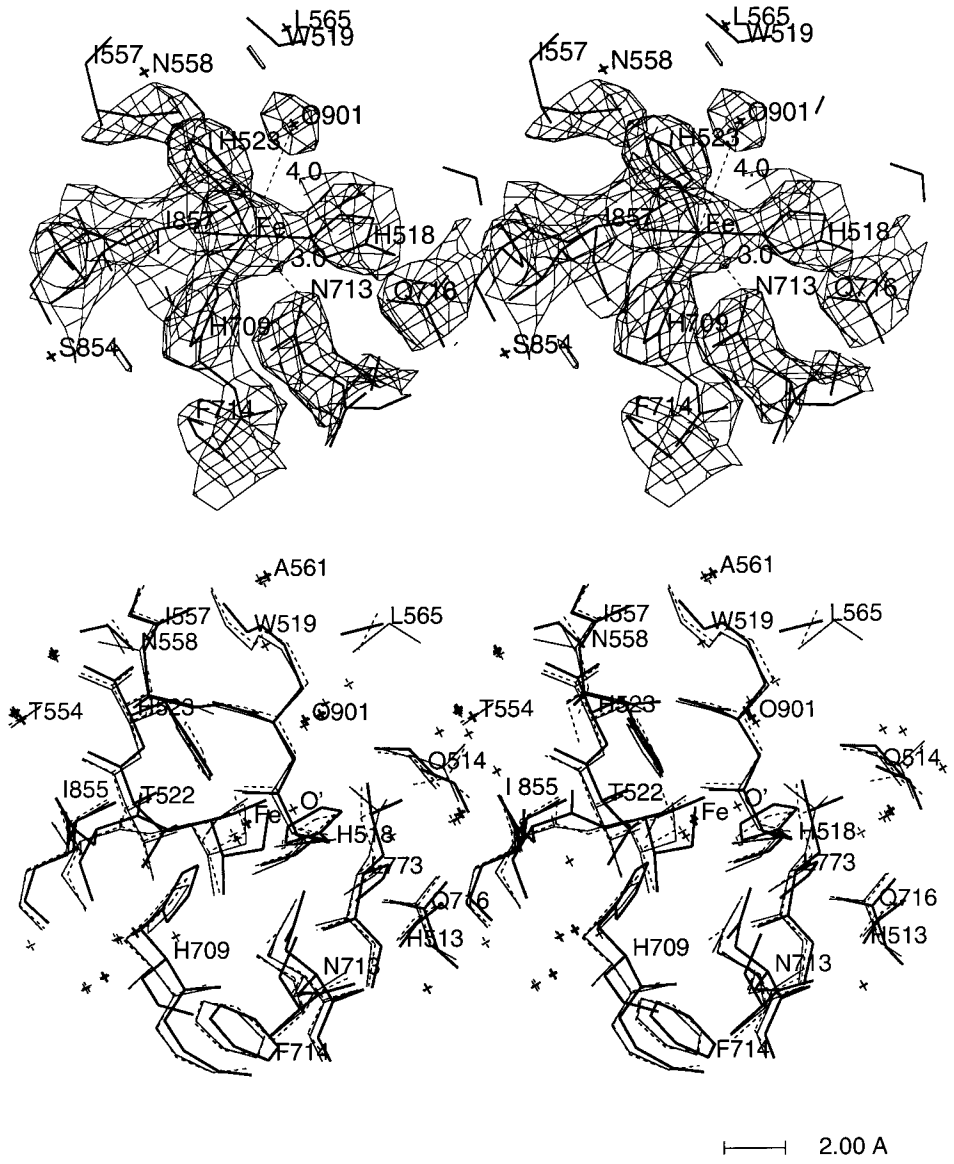

Fig. 4. Iron-binding site. **a** (top): The omit map calculated without Asn713 and Wat901 with superimposed model showing correct positioning of these residues in the nonbounded distance to iron. **b** (bottom): Comparison of L3 structure (bold line) with L1 at room temperature (dashed line) and at 100K (thin line).

H21. The cavities I and II approach the iron-binding site from the direction of His518 and Asn713, whereas cavity III approaches from the Ile857 and His709 side of the coordination sphere.

The number of ligands to the iron[§] in soybean lipoxygenase was for a long time a subject of a heated discussion[3,7] that, upon looking at Figure 4b, proves to be purely a consequence of the use of different ways to define a ligand, and the different assump-

[§]It has been found that iron in its organometallic complexes can be 4, 5, 6, or 7 coordinated, with 6 been observed most often.[33] In diiron containing metalloproteins the iron atoms are six coordinated.[21,34] However, in proteins with nonheme iron as a single metal cofactor, the number of ligands varies from 4, through 5, to 6. An excellent example of the adaptability of the iron coordination sphere has been shown for iron superoxide dismutase. Stoddard et al., 1990[35] reported four ligands to iron arranged in an asymmetric trigonal bipyramid with one axial site unoccupied (all ligands at distances $\geq$ 2.3 Å). The same enzyme, studied at a different pH (pH 7 vs. 4.8) by a different team of researchers was found to have a water molecule as a fifth ligand.[36] Examination of iron(II) and iron(III) superoxide dismutases showed no significant differences in the iron-binding site. However, soaking the crystals of the iron(III) enzyme with sodium azide led to the determination of a structure with azide bound as a sixth ligand in a distorted octahedral geometry at the metal. Because the experiments[36] were conducted by using the same crystals, there can be no doubt that iron can alter and easily rearrange its coordination sphere as it undergoes redox processes.

TABLE I. Selected Hydrogen Bonds and Their Role in the Tertiary Structure of Lipoxygenase

Hydrogen bond		Distance	
Residue 1	Residue 2	(Å)	Its role in the tertiary structure: connects
Iron binding site, NE2 atoms from histidines bind to metal cofactor			
His518 ND1	Gln514 OE1	3.0	
Gln514 NE2	Gln716 OE1	2.8	H9 to H18
Gln716 NE2	Asn713 OD1	2.9	
Asn713 ND2	Leu773 O	2.9	H18 to H21
His523 ND1	Asn558 OD1	2.8	
Asn558 ND2	His523 O	3.0	H9 to H11
His709 ND1	Wat985	2.9	
Other His in the conserved cluster			
His513 NE2	Val712 O	2.7	H9 to H18
	Val372 O	2.7	H9 to loop between H6 and E12
His513 ND1	Wat936	2.7	
His541 ND1	Glu663 OE2	2.9	H10 to H17
Glu663 OE2	Arg180 NH2	2.8	H17 to H1
His541 NE2	Tyr652 OH	3.4	H10 to loop between H15 and H16
Tyr652 OH	Asp661 OD1	2.8	H16 to H17
His550 NE2	Wat1112	2.8	loop between H10 and H11
Wat1112	Trp643 NE1	3.2	to H15
His550 ND1	Asn853 O	2.7	and to C_t

C_t stands for C-terminal coil, H for helix, Wat for water molecule. The term "conserved His cluster" relates to His: 513, 518, 523, 541, 550, and 709 present in all lipoxygenases with one exception: His523 is Gln in *soyL2*.

tions made during refinement of the structure.¶ Superposition of L1 and L3 (based on the best fit of Cα, mean rms deviation L1 (RT to LT)** = 0.8 Å) shows the same spatial arrangements of the six residues around Fe. The only significant differences concern the structure described at approximately 200° lower temperature (100K), where the plane of an imidazole ring of His499 (518 in L3) adopts a different orientation and the water was located closer to Fe (2.5 Å) and accompanied by a second one. It is not surprising to find a different number and location of the solvent molecules in the structures that differ approximately 200° in temperature and 1.2 Å in resolution. However, in both cases (L1, L3) the solvent molecule occupies the space designated for the sixth ligand of iron, lies in the hydrophobic cavity, and does not form any hydrogen bonds with the surrounding amino acids (Fig. 5). Selected distances and O are marked to visualize the size of this space and the positions of the two water molecules (841 and 842) localized in L1 (LT).Substitutions L1/L3—Thr259/Ile277, Ile547/Val566, and Ile552/Val571—make this cavity more spacious and, by removing Thr, more hydrophobic. Both factors might contribute to stereoselectivity that for L3 is less stringent than for L1.[12] Also noteworthy is a possible role for Trp519 and Phe714 in π-π interactions and assistance in the withdrawal of the water molecule. The NE1 atom of Trp519 makes a hydrogen bond with OH Tyr232. These two residues are conserved in plant lipoxygenases but are Leu (and one Gln in *musplat12*), respectively, in the mammalian enzymes. There is plenty of space around Trp519 for this residue to swing its side chain and, for instance, interact with the water next to iron, or with π electrons from the double-bond system of the fatty acid. So it is reasonable to hypothesize that this residue might play the role in substrate positioning in plant lipoxygenases. Phe714 plays a supportive role shielding Asn713 and is involved in stacking interactions with His776 and Tyr782. This Asn/Phe/His/Tyr cluster is conserved in sequences of 18 of 20 plant species (position 713 (in L3) is His in *tomat2*, 776 is Thr in *potatA*) changing to a variety of other combinations (713 often as His) in the rest of lipoxygenases. Again, this might be an indication that Phe714 is necessary for the long-range interactions

¶The distance criterion rules out Asn and the solvent molecule as the iron ligands. On the other hand, ligands in proteins could show higher variability than small molecule structures. For instance, His26 in superoxide dismutase shows large variations in the distance to iron (*Escherichia Coli*: Fe-N = 2.2 Å,[36] *Pseudomonas ovalis* (Fe-N = 2.6 Å[35]). Whether such differences are actual differences, or whether they may result from different resolution, quality of data, and different ways of refinement, is starting to be acknowledged and discussed in the recent literature.[7]

**Where abbreviations RT and LT stand for room temperature (PDB entry 2SBL[6]) and low temperature data.[7] E.S.J. thank B. Stec and W. Minor for providing coordinates and temperature factors corresponding to the unpublished results of the isotropic refinement of L1 (LT, not the final results), for the purpose of this comparison. B_{avg} (Å^2) for the side chains of the selected residues in L1 molecule A and B, and in L3: His499 A/B/His518-28/29/27, His504 A/B/His523-22/21/18, His690 A/B/His709-19/11/18, Asn694 A/B/Asn713-16/13/14. Similar tendency (but of a lower magnitude) is observed in L1 at low temperature (100K), where corresponding values are as follows: His499-17, His504-15, His690-12, and Asn694-13 Å^2.

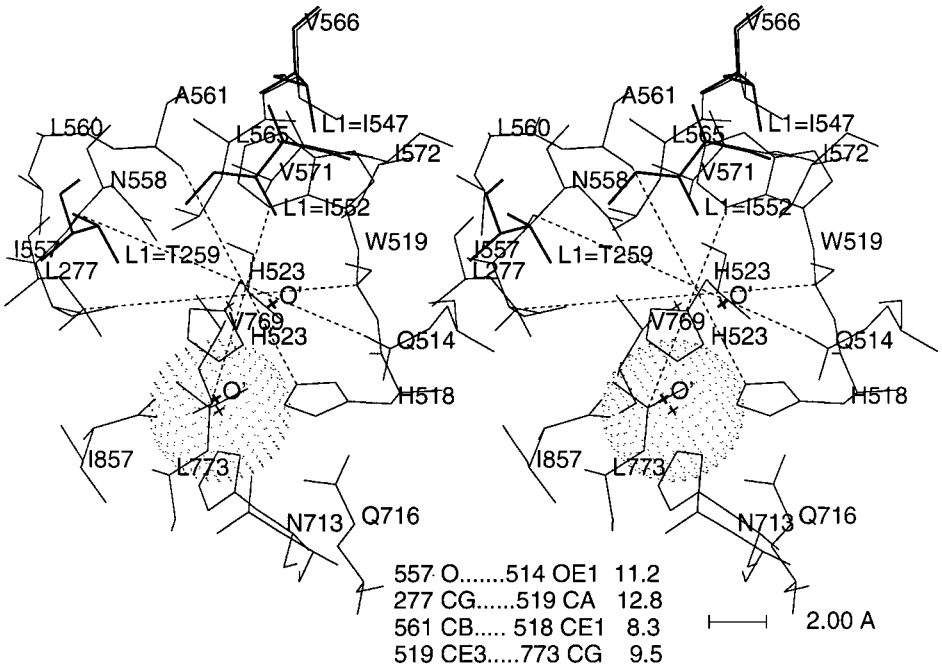

Fig. 5. The water environment at iron-binding site. Center at Wat901, L1 residues Thr259, Ile547, Ile552, and O' bold line, selected distances (dashed lines) marked to illustrate the size of this space.

at the active site, other than direct electron transfer Fe-C(substrate),[37,38] in the redox reactions regulated by plant lipoxygenases.

In contrast to L1 and L3 at RT, His499 at LT does not participate in a hydrogen-bonding network His499/518...Gln495/514...Gln697/716...Asn694/713 (Table 1). It does support our earlier observation[16] that this His shows higher mobility than the other two histidines ligated to iron. In all four known molecular structures of soybean lipoxygenase isoenzymes (i.e., His499 in L1 molecule A and molecule B at RT, His499 in L1 at LT, and His518 in L3) an average B-factor for the side chain of this histidine is greater (6–18 Å^2 at RT and 2–5 Å^2 at LT)** than B_{avg} of the other residues surrounding the iron. Also, His367 in human 5-lipoxygenase, corresponding in a sequence alignment to His499/518 in L1/L3 soybean lipoxygenases, was found not to be crucial for the iron binding, but necessary for enzyme activity.[39] Site-directed mutagenesis studies have subsequently shown that the asparagine is not required for iron incorporation into the protein expressed in *E. coli* but that this residue is critical to the catalytic activity.[26] Asn713Ser and Asn713Ala mutants of L3 have no detectable catalytic activity. The Asn713His mutant, however, shows catalytic behavior similar to that of the wild-type protein, whereas the same mutation in L1 (Asn694His) leads to an enzyme of very limited activity (where His694, like Asn before, was found at nonbinding distance, 2.8 Å from the iron).[40] These observations suggest that His518 and Asn713, strategically located at the junction between the cavities, might have the roles of traffic controllers during catalysis.

Among residues connecting 518 to 713 through the chain of the hydrogen bonds, His518 and Gln716 are conserved (except Leu at Gln position in *tomato2*), Asn713 is conserved in plant (except *tomato2*), mammalian-5 and some -12, but is His in other -12 and -15 lipoxygenases (and *tomato2*). Gln514 is present in plant (except *rice2*), mammalian-5 and *musepi*, and is Glu in the rest of enzymes. Substituting Asn713 by His causes no change in activity in L3,[26] but L1 shows only limited activity.[40] Histidine fits in the space occupied by Asn; they both *can* form hydrogen bonds, but the Asn/His replacement changes the delicate balance of charges in the protein. It affects L1 and L3 in the same way; therefore, the reason for that different behavior must not be in the Asn/His mutation itself, but in the other sequential and conformational changes in the residues participating in catalysis of the given isoenzyme. The prime candidates are the sequential changes near the iron, in the cavities leading to it and near them, and next to the specificity pocket. Those changes are illustrated in Figure 6, and they all can have more or less of a direct impact on catalysis by altering the volume and openings of the cavities, local charges, and hydrophobicity.

Cavities

Two of the cavities coincide with those described in L1 as cavity I and II.[6,7] The third runs from the iron site to the interface between the bulk of the L3 molecule and the N-terminal β-barrel. Cavity III, the iron site, and cavity II form the longest passage throughout the molecule, which distinguishes L3 from L1. Regions 2 and 3 (yellow and red in Fig. 1), form a cap over helical region 5 (gray in Fig. 1) that, like a butterfly clip, covers the groove above the iron-binding site (between H11 and H21) with H2 (Figs. 1 and 3b). This cap extending from H17 on one side, to H20 on the other, may (through its flexible loops at the ends) control access to cavities II and III. It also contains a scissile bond (Arg336Thr337) that, when proteolyzed, might expose the iron cofactor. The other connection between the surface and the iron is a shorter funnel-shaped cavity I having loops E12→H7 and H13→H14 at its entrance. In comparison between L1 and L3 cavities I, II, and "the wall" separating them, have structural and sequential differences, where the most prominent are (L1/L3): Trp555/Gln574 in the specificity pocket, Pro559/Trp578 in the loop H12→H13, accompanied by Ile412/Pro432 and Phe413/Ile433 in E13→H8. The adjacent fragments of L3 (H8, H12→H13) do not match L1 as closely as elsewhere, but the interior of cavity I retains its shape. At the entrance, however, the long, flexible coil E12→H7 contains Lys388 (Asp370 in L1) that reaches across and can form a salt bridge with Asp592 (after H13). The entrance to cavity II is more open in L3 due to the substitutions His730/Pro749 (located at the beginning of H20) and Ile487/Val506 (in H9). This cavity is blocked in the middle by a salt bridge formed by Arg726 and Asp509, that, on the other side, binds to Tyr409/His429 (Fig. 6). This change (Tyr to His in the loop E13→H8) together with another one—Ser747/Asp766 (in H21)—provide the additional charges that might promote rearrangement of Arg726 influencing the flow in that cavity. Comparison of lipoxygenase sequences shows that Arg (726 in L3) is typical for plants, whereas Ala or Gly is typical of mammals. Asp (509 in L3) is conserved in all, but His429 occurs in 13 of 20 plant enzymes while staying aromatic and uncharged (Tyr or Phe) in the remaining 7 plant and 13 mammalian enzymes. Acidic Asp766 (and one Glu) occurs in 50% of plant enzymes (the rest of them having Gly, Val or Ser), changing to basic His in mammalian-5 while staying neutral in the other -12 and -15. Examination of the possible conformers of Arg726 shows that one of them can form a salt bridge with Asp766 (replacing Wat1103), whereas another (it would replace Wat940) points to the cluster of Glu363...Arg366Glu367 (Fig. 7a) and forms stacking interaction with an aromatic ring of Tyr719. In either case, this passage opens up. This Glu...ArgGlu cluster (363,366,367 in L3) is conserved in plant enzymes (except *arabido2* where Glu367 corresponds to Gln), and not present (substituted by neutral residues) in mammalian lipoxygenases, where Arg (726 in L3) is replaced by Ala or Gly as well. These observations suggest that Arg726 may regulate the flow in this passage by switching from one conformer to another, forming salt bridges with different residues, depending on the stage of catalysis and enzyme involved.

Another interesting place in the L3 structure is a crevice between the N_t-β-barrel and the ends of helices H2, H11, and H21. A comparison of L1 and L3 shows alterations in the sequence (Asn245/Ala263, Leu246/Phe264, Ala254/Phe272, Glu256/Tyr274, Ile257/Tyr275, and others less drastic) and the structural changes in that region that open up the third cavity leading to the metal cofactor. The route to the iron from this side (approximately 15 Å) is closed in L1 by the salt bridge Glu256...His248 (corresponds to Thr274, His266 in L3) that is not present in L3, Fig. 6b. Cavity III is formed by the loop Asp255 to Lys278 (NZ Lys278...O Asn254 = 3.2 Å), a fragment of H11: Asp552 to Leu560, the loop after H21: Leu773 to Val 781, C_t-terminal: Pro852 to Ile857, and the residues Glu197, Tyr150, Glu124, Lys21, Asp25Val26Asn27 from N_t-domain, that, together with Tyr275, Lys278, and Asp255, make a mouth of this cavity (approximately 9 Å wide). Residues His266...Asp779...Arg552...Phe264 separate the bottom of this cavity from the solvent in a crevice formed by the opposite side of the N_t-β-barrel: Phe126 and Asn146, and the loop 779→788 (after H21). The entrance to cavity III is in the vicinity of the disordered insertion loop that, if extended, would be large enough to cover it. This loop might be visible in LT analysis. However, it is disordered in the crystal, and then it is highly probable for this fragment to be flexible in vivo, where catalysis occurs at ambient temperature. That suggests that the approach to the iron site through this passage might be regulated by this loop. One can also anticipate that different routes are used by the approaching substrate and the product leaving the catalytic site. Analysis of the structural differences between L1 and L3 suggests that there are more options and flexibility to accommodate the fatty acid in the L3 isozyme. This characteristic might explain why this enzyme produces a greater variety in the mixture of products.

Modeling of Linoleic Acid Into L3 Structure

Linoleic acid, a long and flexible molecule, was shown to adopt an extended conformation in its crystallized form.[41] Starting with this conformation, we adjusted the molecule to the shape of the cavities

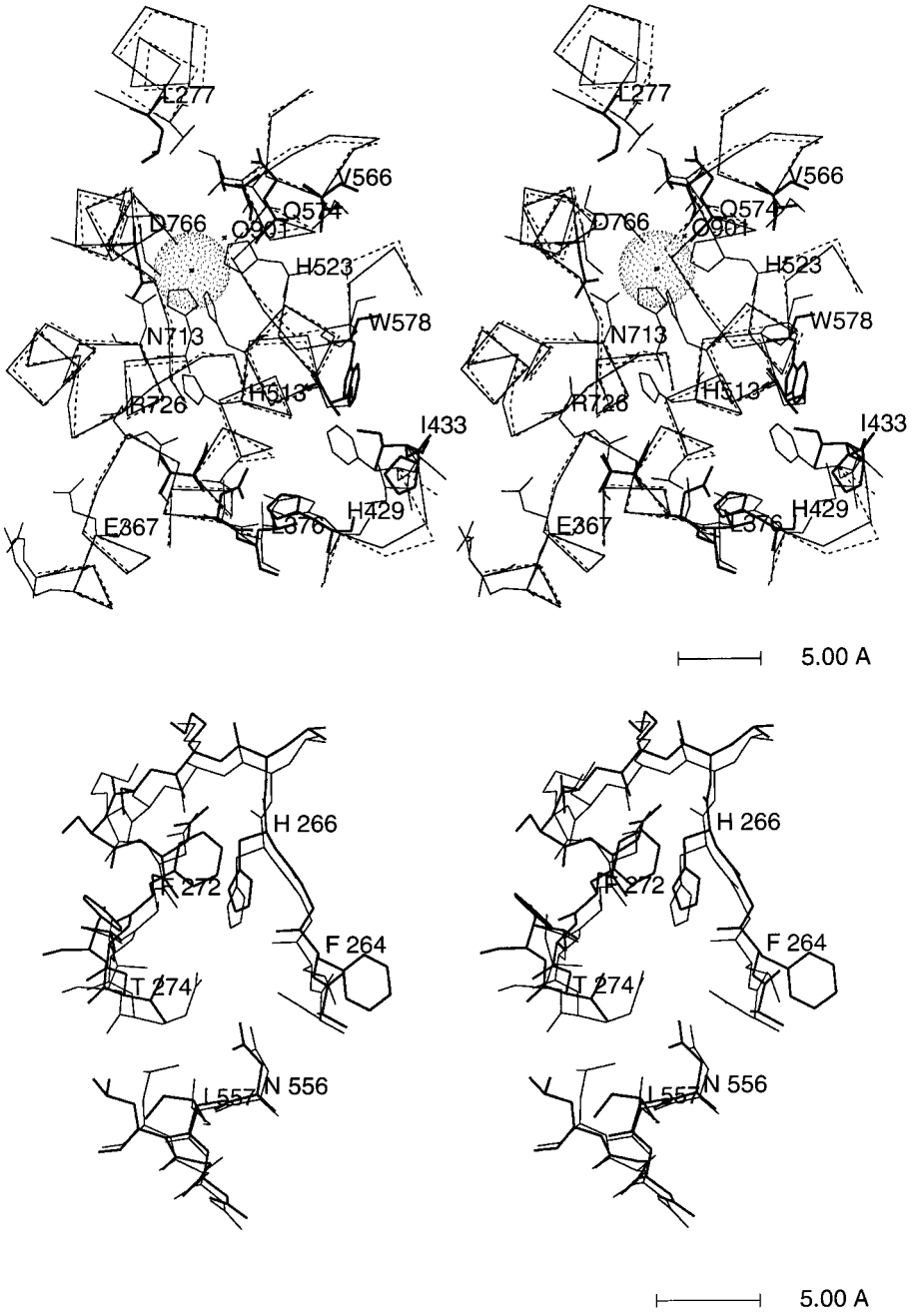

Fig. 6. Sequential and conformational differences between L1 and L3 in the iron neighborhood. **a** (top): Cavity II: Thin line: Cα backbone of L3 structure and chosen residues common for both L1 and L3, or present in L1 only; bold line: amino acid present in L3; dashed line: Cα backbone of L1. The following mutations are present in this figure (L1/L3, listed from top): **H2**: Thr259/Leu277; **H21**: Ser747/Asp766; **H11** to **H13**: Ile547/Val566, Ile552/Val571, Thr555/Gln574, Pro559/Trp578; **H9**: Ile487/Val506, Met497/Val516; **H6** to **E12**: Cys357/Asn375, Val358/Leu376; loop **E13** to **H8**: Tyr409/His429, Ile412/Pro432, Phe413/Ile433. **b** (bottom): Cavity III: A fragment showing a salt bridge in L1 (thin line) and the local changes in L3 (bold line).

in L3, by changing the torsional angles around single bonds. No alterations were made to the L3 structure for the purpose of this modeling. Linoleic acid was placed in an available space near the iron site, assuming that 1) it can displace water molecules (present in the L3 model), 2) its terminal carboxylic group can bind to iron (in place of Wat901), 3) the aliphatic parts are near the hydrophobic side chains, and 4) there might be long-range electron transfer involved in catalysis.

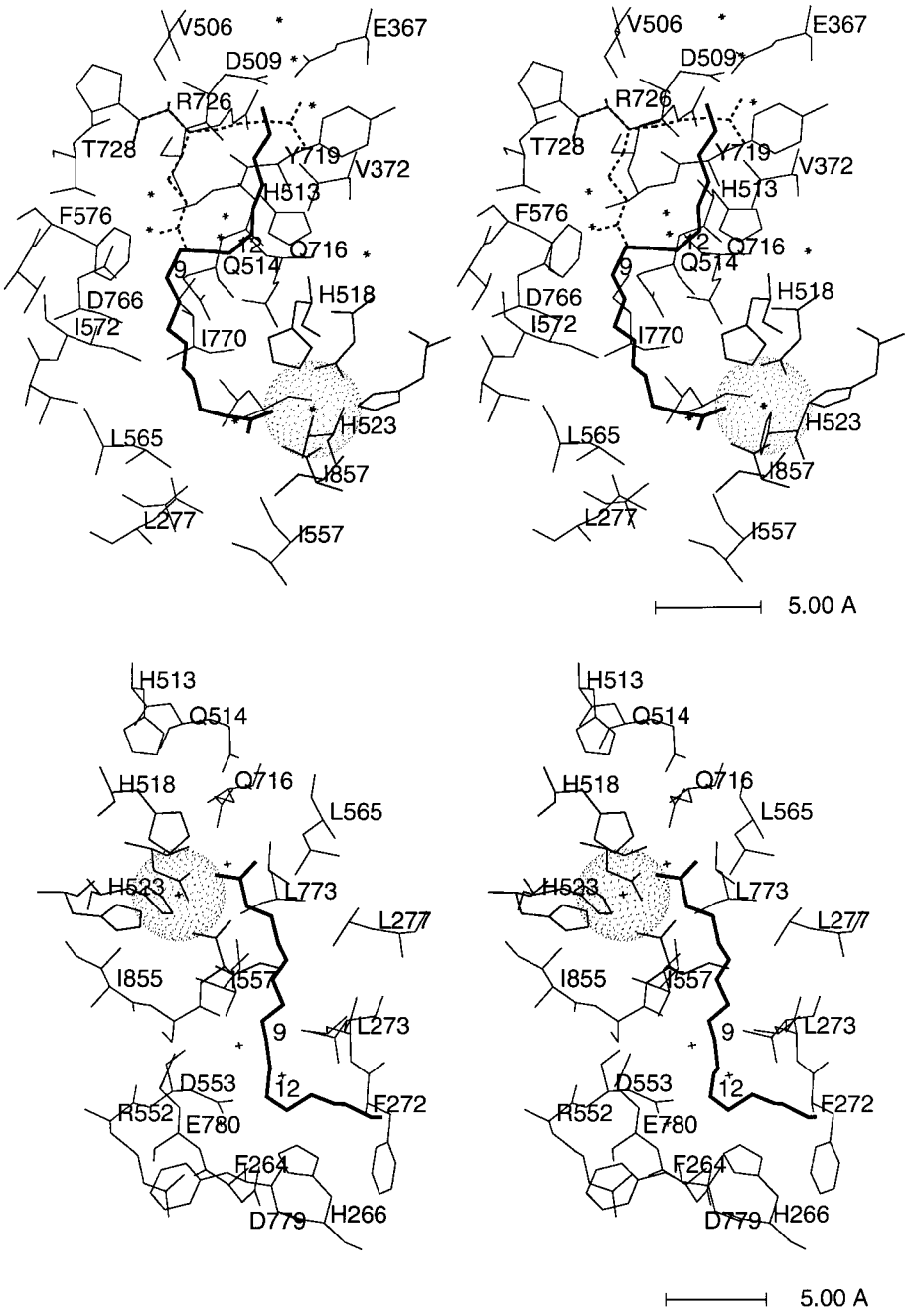

Fig. 7. Detailed views showing L3 backbone with selected residues (thin line), and linoleic acid built into L3 structure in two possible orientations (bold line): from Fe around His513 and toward Arg726 (**a**, top) and from Fe toward His266 and N_t-domain (**b**, bottom).

Assumptions 2 and 4 allow the investigation of alternative models to those proposed before for L1 and human lipoxygenases[42] (where the 1,4-diene system was placed near iron with the carboxyl and methyl terminals stretching out into suitable pockets). Carboxylic groups are commonly observed ligands to iron in metal complexes.[33] The X-ray structures of lipid-binding proteins give us examples illustrating three different ways of FA binding. Two of them show FA in "curled" or "extended" form at the end of the β-barrel, with the carboxylic end inside the barrel, and the hydrophobic chain toward adja-

cent, short helices (Protein Data Bank at Brookhaven, entries 1ADL[43] and 1LID[44] can serve as examples). The third example[45] shows FA moiety buried between two long helices, with the carboxylic end of oleate sticking out into solvent. In lipoxygenase the distance from iron to β-barrel (at either end of the molecule) would be approximately 30 Å, and in case of the internal cavities in the helical domain, approximately 10 Å. The long-range electron transfer has been widely discussed in the literature[46,47] and observed in other cases of redox reactions involving metalloenzymes.[48–50††] Although we do not have any experimental data supporting this mechanism in lipoxygenases, the possibility seems worthy of exploration, although in this modeling we limited it to the vicinity of iron and cavities II and III.

Figure 7 shows two models of L3:linoleic acid complexes (the short contacts present in a few places could be easily changed by altering the torsional angles of the side chains involved). In the first case, Fig. 7a, C2 to C8 go along Leu773, Ile770, Leu565, Ile572; the double bonds C9=C10-C11-C12=C13 bend over Gln514...Gln716, with Phe576 close to C9, His513 next to C13, and Arg726 (alternative rotamer) and Asp766 for assistance, and the tail of the fatty acid is directed toward Val372 and Val506. In a second case, Fig. 7b, C2 to C8 come in contact with Leu565, Leu773, Leu277, Ile857, Ile557, Leu273-Thr274, the double bonds between Leu273 and Asp553, with C13 next to His266, and the tail of the fatty acid toward Val26. It is not difficult to imagine that C9 can come close to His266 and Phe272 (upon slight movement of the enzyme C-terminal to make the 852–857 loop tighter), if the fatty acid positions differently in this cavity with the tail stretched toward Arg552. C9 can also be brought to the proximity of His776. This would require a relocation of L3-C-terminal to the Wat901 site. The fatty acid could then bind to iron next to Asn713 and His709 and lean against Phe714 and His776. That would promote peroxidation at C9 (while C13 would be near His266, Arg552, and Asp779).

These models and the geometrical considerations presented above, suggest that the residues His513, His266, His776, Phe264, Phe272, Phe576, Phe714, Arg552, Arg726, Asp 766, Asp779 might be of assistance in catalysis.

The iron site in lipoxygenase would appear to be fully capable of adapting to the steric and electronic demands of catalysis, which include positioning two substrates and facilitating the redox chemistry. The participation of the C-terminal carboxylate group of Ile857 as a ligand, attached as it is through a long, flexible arm, could (in conjunction with the large surrounding cavity) provide for movement within the active site, as it adopts the arrangement best suited to the current stage of substrate and/or product binding and electron transfer.

SUMMARY

Comparison of the L1 and L3 isozymes of soybean lipoxygenase reveals the following. 1) The isozymes have generally the same structure and the same organization of domains within the molecule, with rms deviation between Cα backbones of 1 Å. The barrel-like shape and other topological features near region 4 (346–488) suggest that this part, as N_t-barrel, might play some role in molecular recognition during catalysis and/or proteolysis. 2) The iron site in both soybean lipoxygenases appears to have the same geometry, except for His518, which shows greater mobility than the other ligands. 3) The L3 molecule has three cavities connecting the iron site with the surface of the molecule. The entrance to cavity III (roughly 15 Å from Fe), located in the interface between regions 1, 2, and 3, is closed in L1 by the salt bridge that is not present in L3. Cavity III, together with cavity II, form a continuous passage winding through the molecule. Region 3 covers the groove with the iron site and can control cavities II and III. Region 4 borders cavities I and II. Regions 3 and 4 are linked in L3 by a proline triad 346-347-348, not present in L1 (where Glu329 is in place of Pro347). These prolines (marked as a white fragment between "red" and "blue"; Figs. 1, 8) might work like a hinge providing assistance in the movement of the different parts of the molecule (if there is such movement involved during substrate binding). Two or three Pro are present in this place in 80% of plant enzymes (mammalian enzymes do not have this fragment, 336→353 in L3 numbering). Any change in relative orientation of regions 1–5 would have an impact on the accessibility of the iron site. 4) Modeling studies of binding linoleic acid to L3 provide insight into the possible nonorgano-iron pathway for the redox reaction. The models suggest that the following residues (Fig. 8), His:266, 513, 776, Phe:264, 272, 576, 714, Trp519, Arg:552, 726, Asp: 766, 779, and Lys278 might be of value for catalysis.[‡‡] Their importance can be tested by the site directed mutagenetic experiments affecting these

[††]The observations made for R1-R2 complex in ribonucleotide reductase led to a conclusion describing an *inter*molecular electron transfer from one protein with an iron site to another protein with a substrate-binding site (where a hydrogen abstraction occurs) over the distance of 35 Å.[48]

[‡‡]The latest literature[52] provides additional insight into arachidonic acid binding to human 15-lipoxygenase. The results of a site-directed mutagenesis point out that the charged residue, Arg402, and the aromatic residue, Phe414, are both critical for catalysis (in soybean lipoxygenases they correspond to L1/L3: Leu541/560 and Ile553/572, which are the near neighbors (in space) of Lys260/278 and Trp500/519).

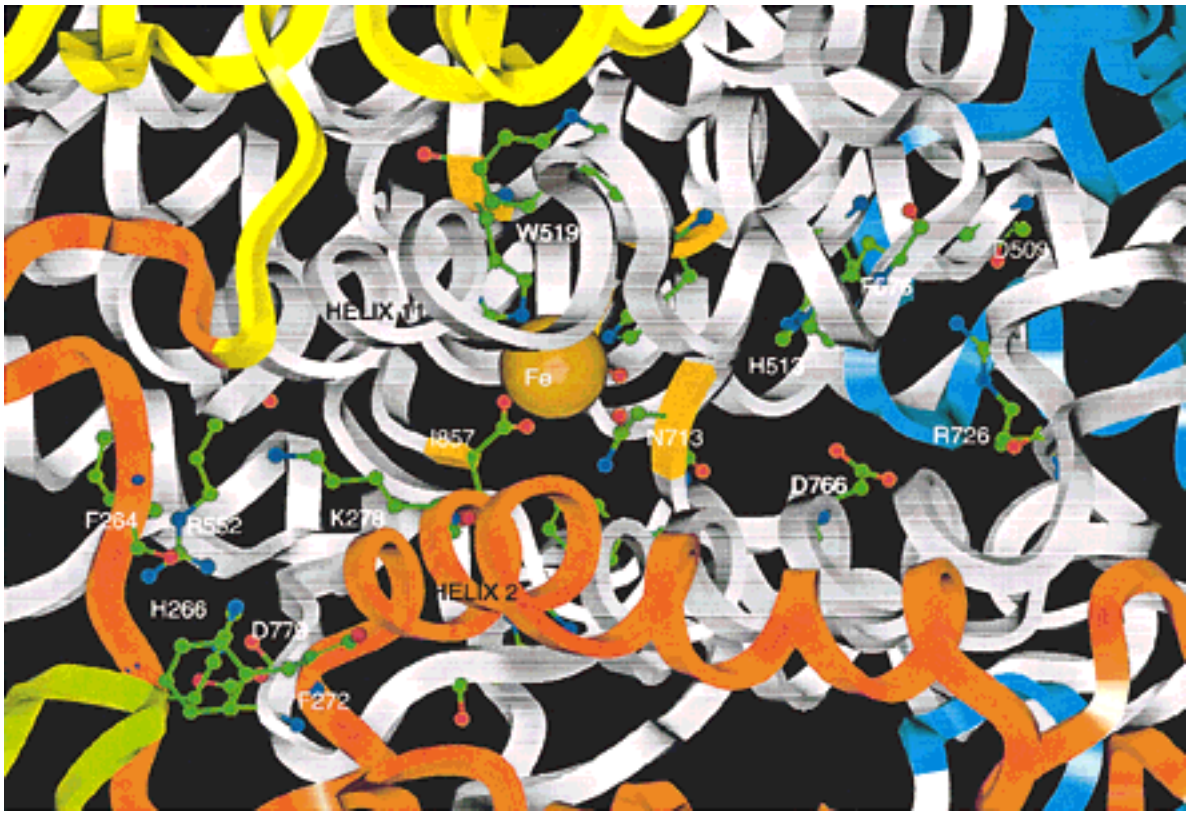

Fig. 8. L3, location of selected residues that might be of importance in catalysis. Orientation and colors the same as in Figure 1.

residues (and others participating in the hydrogen bonds in this vicinity, such as Gln514, Gln716, Ser856, Asp779, Glu780). 5) The L3 structure and electron density map indicate that the salt bridge partitioning cavity II can be open, when an alternative rotamer of Arg726 forms a salt bridge with Asp766 (or Glu367), leaving Asp509 from a former ion pair to interact with His429. The residues Asp766 and His429 are sequential changes in relation to L1.

The presence of cavity III, possible opening of cavity II and, in general, more room in the passages for substrate/product, may provide an explanation for the different regioselective and stereoselective characteristics of catalysis by the L1 and L3 soybean isozymes.

ACKNOWLEDGMENTS

The data have been deposited (1LNH) with the Protein Data Bank, Chemistry Department, Brookhaven National Laboratory, Upton, NY 11973. This work was supported by NIH Grant GM-46522 to Max O. Funk and Ewa Skrzypczak-Jankun and NIH Grant GM-44692 to L. Mario Amzel).

REFERENCES

1. Samuelsson, B., Dahlen, S.E., Lindgren, J.A., Rouzer, C.A., Serhan, C.N. Leukotriens and lipoxins—Structures, biosynthesis, and biological effects. Science 237:1171–1176, 1987.
2. Funk, M.O., Carroll, R.T., Thompson, J.F., Sands, R.H., Dunham, W.R. The role of iron in lipoxygenase catalysis. J. Am. Chem. Soc. 112:5375–5376, 1990.
3. Nelson, M.J., Seitz, S.P. The structure and function of lipoxygenase. Curr. Opin. Struct. Biol. 4:878–884, 1994 and references cited therein.
4. Nelson, M.J. Evidence for water coordinated to the active site iron in soybean lipoxygenase-1. J. Am. Chem. Soc. 110:2985–2986, 1988.
5. Scarrow, R.C., Trimitsis, M.G., Buck, C.P., Cowling, R.A., Nelson, M.J. X-ray spectroscopy of the iron site in soybean lipoxygenase-1: Changes in coordination upon oxidation or addition of methanol. Biochemistry 33:15023–15035, 1994.
6. Boyington, J.C., Gaffney, B.J., Amzel, L.M. The three-dimensional structure of an arachidonic acid 15-lipoxygenase. Science 260:1482–1486, 1993.
7. Minor, W., Steczko, J., Stec, B., Otwinowski, Z., Bolin, J.T., Walter, R., Axelrod, B. Crystal structure of soybean lipoxygenase L-1 at 1.4 Å resolution. Biochemistry 35:10687–10701, 1996.
8. Ford-Hutchinson, A.W., Gresser, M., Young, R.N. 5-Lipoxygenase. Annu. Rev. Biochem. 63:383–417, 1994.
9. Siedow, J.N. Plant lipoxygenases—Structure and function.

Annu. Rev. Plant Physiol. Plant Mol. Biol. 42:145–188, 1991.
10. Miller, D.K., Gillard, J.W., Vickers, P.J., Sadowski, S., Leveille, C., Mancini, J.A., Charleson, P., Dixon, R.A.F., Ford-Hutchinson, A.W., Fortin, R. Identification and isolation of a membrane-associated protein necessary for leukotriene production. Nature 343:278–281, 1990.
11. Draheim, J., Carroll, R.T., McNemar, T.B., Dunham, W.R., Sands, R.H., Funk, M.O. Lipoxygenase isoenzymes—A spectroscopic and structural characterization of soybean seed enzymes. Arch. Biochem. Biophys. 269:208–218, 1989.
12. Andre, Jon C., Funk, Max O. Determination of stereochemistry in the fatty acid hydroperoxide products of lipoxygenase catalysis. Anal. Biochem. 158:316–321, 1986.
13. Gardner, H.W. Soybean lipoxygenase-1 enzymically forms both (9S)- and (13S)-hydroperoxides from linoleic acid by a pH-dependent mechanism. Biochim. Biophys. Acta 1001: 274–281, 1989.
14. Stallings, C.W., Kroa, B.A., Carroll, R.T., Metzger, A.L., Funk, M.O. Crystallization and preliminary X-ray characterization of a soybean seed lipoxygenase. J. Mol. Biol. 211:685–687, 1990.
15. Kroa, B.A., Funk, M.O., Jr. Preliminary crystallographic analysis of new prismatic soybean lipoxygenase crystals. American Crystallographic Association, Annual Meeting, Toledo, July 21–26, 1991, PG18, p. 106.
16. Skrzypczak-Jankun, E., Funk, M.O., Jr., Boyington, J.C., Amzel, L.M. Lipoxygenase—A molecular complex with a non-heme iron. Collected materials of 9th Symposium on Organic Crystal Chemistry, Poznan-Rydzyna, Poland, 23–27 August, 1994 in J. Mol. Struct. 374:47–52, 1996.
17. Funk, M.O., Jr., Carroll, R.T., Thompson, J.F., Dunham, R.W. The lipoxygenases in developing soybean seeds, their characterization and synthesis in vitro. Plant Physiol. 82:1139–1144, 1986.
18. Navaza, J. AMoRe: An Automated Package for Molecular Replacement. Acta Crystallogr. A50:157–163, 1994.
19. Brünger, A.T. X-PLOR version 3.1. A System for X-ray Crystallography and NMR. New Haven, CT: Yale University Press, 1992.
20. Sack, J.S. CHAIN—A crystallographic modeling program. J. Mol. Graphics 6:224–225, 1988.
21. Mashuta, M.S., Webb, R.J., McCusker, J.K., Schmitt, E.A., Oberhausen, K.J., Richardson, J.F., Buchanan, R.M., Hendrickson, D.N. Electron transfer in FeIIFeIII model complexes of iron-oxo proteins. J. Am. Chem. Soc. 114:3815–3827, 1992.
22. Tesmer, J.J.G., Muchmore, C., Steczko, J., Axelrod, B., Smith, J.L. Low temperature data collection of soybean lipoxygenase. American Crystallographic Association, Annual Meeting, Toledo, July 21–26, 1991, PG17, p. 105.
23. Skrzypczak-Jankun, E., Bianchet, M.A., Amzel, L.M., Funk, M.O. Flash-freezing causes a stress-induced modulation in a crystal structure of soybean lipoxygenase L3. Acta Crystallogr. D52:959–965, 1996.
24. Steczko, J., Minor, W., Stojanoff, V., Axelrod B. Crystallization and preliminary X-ray investigation of lipoxygenase-3 from soybeans. Protein Sci. 4:1233–1235, 1995.
25. Kabsch, W., Sanders, C. Dictionary of protein secondary structure: Pattern recognition of hydrogen-bonded and geometrical features. Biopolymers 22:2577–2637, 1983.
26. Kramer, J.A., Johnson, K.R., Dunham, W.R., Sands, R.H., Funk, M.O., Jr. Position 713 is critical for catalysis but not iron binding in soybean lipoxygenase 3. Biochemistry 33:15017–15022, 1994.
27. Shibata, D., Steczko, J., Dixon, J.E., Andrews, P.C., Hermodson, M., Axelrod, B. Primary structure of soybean lipoxygenase L-2. J. Biol. Chem. 263:6816–6821, 1988.
28. Flores, T.P., Orengo, C.A., Moss, D.S., Thornton, J.M. Comparison of conformational characteristics in structurally similar protein pairs. Protein Sci. 2:1811–1826, 1993.
29. Monaco, H.L., Zanotti, G. Three-dimensional structure and active site of three hydrophobic molecule binding proteins with significant amino acid sequence similarity. Biopolymers 32:457–465, 1992.
30. Steczko, J., Donoho, G.A., Dixon, J.E., Sugimoto, T., Axelrod, B. Effect of ethanol and low-temperature culture on expression of soybean lipoxygenase L-1 in Escherichia coli. Protein Expr. Purif. 2:221–227, 1991.
31. Ramachandran, S., Caroll, R.T., Dunham, W.R., Funk, M.O., Jr. Limited proteolysis and active-site labeling studies of soybean lipoxygenase 1. Biochemistry 31:7700–7706, 1992.
32. Richards-Sucheck, T.J., Ramachandran, S., Skrzypczak-Jankun, E., Wheelock, M.J., Funk, M.O., Jr. Catalysis sensitive conformational changes in soybean lipoxygenase revealed by limited proteolysis and monoclonal antibody experiments. Biochemistry 34:14868–14873, 1995.
33. Allen, F.H., Davies, J.E., Galloy, J.J., Johnson, O., Kennard, O., Macrae, C.F., Mitchell, E.M., Mitchell, G.F., Smith, J.M., Watson, D.G. The development of version 3 and 4 of the Cambridge Structural Database System. J. Chem. Info. Comp. Sci. 31:187–204, 1991. Cambridge Structural Database, version April 1996.
34. Sträter, N., Klabunde, T., Tucker, P., Witzel, H., Krebs, B. Crystal structure of a purple acid phosphatase containing a dinuclear Fe(III)-Zn(II) active site. Science 268:1489–1492, 1995.
35. Stoddard, B.L., Howell, P.L., Ringe, D., Petsko, G.A. The 2.1 Å resolution structure of iron superoxide dismutase from *Pseudomonas ovalis*. Biochemistry 29:8885–8893, 1990.
36. Lah, M.S., Dixon, M.M., Pattridge, K.A., Stallings, W.C., Fee, J.A., Ludwig, M.L. Structure-function in *E. coli* iron superoxide dismutase: Comparison with the manganese enzyme from *T. Thermophilus*. Biochemistry 34:1646–1660, 1995.
37. Corey, E.J., Nagata Ryu. Evidence in favor of an organoiron-mediated pathway for lipoxygenation of fatty acids by soybean lipoxygenase. J. Am. Chem. Soc. 109:8107–8108, 1987.
38. Nelson, M.J., Seitz, S.P., Cowling, R.A. Enzyme-bound pentadienyl and peroxyl radicals in purple lipoxygenase. Biochemistry 29:6897–6903, 1990.
39. Zhang, Y-Y., Lind, B., Radmark, O., Samuelsson, B. Iron content of human 5-lipoxygenase, effects of mutations regarding conserved histidine residues. J. Biol. Chem. 268:2535–2541, 1993.
40. Lewinski, K., Steczko, J., Holman, T., Sigal, E., Stec, B., Axelrod, B., Minor, W. The crystal structure of Asn694His mutant of L-1 isoenzyme of soybean lipoxygenase. XVII Congress and General Assembly of the International Union of Crystallography, August 8–17, 1996, Seattle, WA. Collected Abstracts, PS04.02.49, p. C-580.
41. Ernst, J., Sheldrick, W.S., Fuhrhop, J.-H. Die Strukturen der essentiellen ungesättigten Fettsäuren, Kristallstruktur der Linolsäure sowie Hinweise auf die Kristallstrukturen der α-Linolensäure und der Arachidonsäure. Z. Naturforsch. 34b:707–711,1979.
42. Prigge, S.T., Boyington, J.C., Gaffney, B.J., Amzel, L.M. Structure conservation in lipoxygenases: Structural analysis of soybean lipoxygenase-1 and modeling of human lipoxygenases. Proteins: Struct. Funct. Genet. 24:275–291, 1996.
43. Lalonde, J.M., Levenson, M., Roe, J.J., Bernlohr, D.A., Banaszak, L.J. Adipocyte lipid binding protein complexed with arachidonic acid: X-ray crystallographic and titration calorimetry studies. J. Biol. Chem. 269:25339–25347, 1994.
44. Xu, Z., Bernlohr, D.A., Banaszak, L.J. The adipocyte lipid-binding protein at 1.6 Å resolution: Crystal structures of the apoprotein and with bound saturated and unsaturated fatty acids. J. Biol. Chem. 268:7874–7884, 1993.
45. Lee, J.Y., Shin, D.H., Suh, S.W. Structural studies on maize lipid transfer protein at 1.2 Å resolution and its oleate complex at 1.3 Å resolution. XVII Congress and General Assembly of the International Union of Crystallography,

August 8–17, 1996, Seattle, WA. Collected Abstracts, PS04.18.07, p. C-244.
46. Curry, W.B., Grabe, M.D., Kurnikov, I.V., Skourtis, S.S., Beratan, D.N., Regan, J.J., Aquino, A.J.A., Beroza, P., Onuchic, J.N. Pathways, pathway tubes, pathway docking, and propagators in electron transfer proteins. J. Bioenerg. Biomembr. 27:285–293, 1995.
47. Lee, H., Faraggi, M., Klapper, M.H. Long range electron transfer along an α-helix. Biochim. Biophys. Acta 1159:286–294, 1992.
48. Ekberg, M., Sahlin, M., Eriksson, M., Sjöberg, B.-M. Two conserved tyrosine residues in protein R1 participate in an intermolecular electron transfer in ribonucleotide reductase. J. Biol. Chem. 271:20655–20659, 1996.
49. Rova, U., Goodtzova, K., Ingemarson, R., Behravan, G., Gräslund, A., Thelander, L. Evidence by site-directed mutagenesis supports long-range electron transfer in mouse ribonucleotide reductase. Biochemistry 34:4267–4275, 1995.
50. Sahlin, M., Lassmann, G., Pötsch, S., Slaby, A., Sjöberg, B.-M., Gräslund, A. Tryptophan radicals formed by iron/oxygen reaction with *Escherichia coli* ribonucleotide reductase protein R2 mutant Y122F. J. Biol. Chem. 269:11699–11702, 1994.
51. Farver, O., Skov, L.K., vanDeKamp, M., Canters, G.W., Pecht, I. The effect of driving force on intramolecular electron transfer in proteins. Studies on single-site mutated azurins. Eur. J. Biochem. 210:399–403, 1992.
52. Gan, Q-F., Browner, M.F., Sloane, D.L., Sigal, E. Defining the arachidonic acid binding site of human 15-lipoxygenase. J. Biol. Chem. 271:25412–25418, 1996.